THE JOURNAL OF BIOLOGICAL CHEMISTRY
Vol. 275, No. 29, Issue of July 21, pp. 22238–22244, 2000

Printed in U.S.A.

Comparing and Contrasting *Escherichia coli* and *Mycobacterium tuberculosis* Mechanosensitive Channels (MscL)

NEW GAIN OF FUNCTION MUTATIONS IN THE LOOP REGION*

Received for publication, April 11, 2000, and in revised form, May 5, 2000
Published, JBC Papers in Press, May 8, 2000, DOI 10.1074/jbc.M003056200

Joshua A. Maurer‡§, Donald E. Elmore‡¶, Henry A. Lester‖, and Dennis A. Dougherty‡**

From the Divisions of ‡Chemistry and Chemical Engineering and ‖Biology, California Institute of Technology, Pasadena, California 91125

Sequence analysis of 35 putative MscL homologues was used to develop an optimal alignment for *Escherichia coli* and *Mycobacterium tuberculosis* MscL and to place these homologues into sequence subfamilies. By using this alignment, previously identified *E. coli* MscL mutants that displayed severe and very severe gain of function phenotypes were mapped onto the *M. tuberculosis* MscL sequence. Not all of the resulting *M. tuberculosis* mutants displayed a gain of function phenotype; for instance, normal phenotypes were noted for mutations at Ala^{20}, the analogue of the highly sensitive Gly^{22} site in *E. coli*. A previously unnoticed intersubunit hydrogen bond in the extracellular loop region of the *M. tuberculosis* MscL crystal structure has been analyzed. Cross-linkable residues were substituted for the residues involved in the hydrogen bond, and cross-linking studies indicated that these sites are spatially close under physiological conditions. In general, mutation at these positions results in a gain of function phenotype, which provides strong evidence for the importance of the loop region in MscL channel function. No analogue to this interesting interaction could be found in *E. coli* MscL by sequence alignment. Taken together, these results indicate that caution should be exercised in using the *M. tuberculosis* MscL crystal structure to analyze previous functional studies of *E. coli* MscL.

The recent crystal structures of two bacterial ion channels, the KcsA potassium channel and the mechanosensitive channel MscL, provide unique opportunities to study ion channel structure-function relationships (1, 2). Concerning the MscL system, recent work has attempted to rationalize the extensive functional studies on *Escherichia coli* MscL (Eco-MscL)[1] in light of the crystal structure, which was obtained for the *Mycobacterium tuberculosis* homologue (Tb-MscL) (3–7). Additionally, several different models for channel opening have been proposed by considering *E. coli* gain of function (GOF) mutations in light of the *M. tuberculosis* crystal structure (1, 3, 8). To evaluate critically these efforts, it is essential to assess the underlying assumption of the portability of Eco-MscL functional data to the Tb-MscL structure. Although the function of the *E. coli* channel has been extensively probed by site-directed and random mutagenesis, analogous studies of the *M. tuberculosis* channel have not been reported (9–15) . Preliminary data have shown that wild type *E. coli* and *M. tuberculosis* MscL are similar electrophysiologically. Both channels exhibit a large single channel conductance, approximately 3.5 nS, and gate with similar tensions in reconstituted liposomes (17).[2] However, the Tb-MscL channel exhibits twice the gating tension of Eco-MscL in *E. coli* spheroplasts (17). This difference may result from protein structural differences, a difference in interactions with lipids, or both.

Sequence alignment is essential to map previously studied *E. coli* GOF mutations onto the *M. tuberculosis* MscL sequence. In this work we report an optimal sequence alignment of 35 MscL homologues and an analysis of regions of conservation and variability. Consistent with previous studies, we find greater conservation in the transmembrane regions than in the loop or intracellular regions. Interestingly, the various channels clearly fall into subfamilies based on sequence similarity, with Eco-MscL and Tb-MscL in different subfamilies.

By using the optimal alignment, we have prepared Tb-MscL analogues of several critical Eco-MscL GOF mutations (Fig. 1*A*). Perhaps surprisingly, we find that several well established Eco-MscL GOF mutants do not translate to the Tb-MscL system. We also directly evaluate a predicted intersubunit hydrogen bond in the Tb-MscL crystal structure (Fig. 1*B*). Cross-linking studies establish that these residues are indeed close in the reconstituted channel and firmly establish the pentameric nature of the channel. Mutations of this pair generally lead to GOF mutants, suggesting an important functional role for this specific region of the channel. Interestingly, no analogous interaction is apparent in the Eco-MscL alignment. Our results indicate that the functional studies performed on the Eco-MscL channel may not map directly onto the Tb-MscL crystal structure.

MATERIALS AND METHODS

Sequence Analysis—Multiple sequence alignments were obtained using alignment of multiple sequences (AMPS) (20, 21), and consensus group analysis was performed using multiple EM for motif elicitation (MEME) (22, 23). The alignment was broken into regions, extracellular

* This work was supported in part by National Institutes of Health Grants NS-34407 and GM-29836. The costs of publication of this article were defrayed in part by the payment of page charges. This article must therefore be hereby marked "*advertisement*" in accordance with 18 U.S.C. Section 1734 solely to indicate this fact.
§ Recipient of National Institutes of Health Predoctoral Trainee Grant GM-08501.
¶ National Science Foundation predoctoral fellow.
** To whom correspondence should be addressed: Division of Chemistry and Chemical Engineering, California Inst. of Technology, 164-30, Pasadena, CA 91125. Tel.: 626-395-6089; Fax: 626-564-9297; E-mail: dad@igor.caltech.edu.

[1] The abbreviations used are: Eco-MscL, large mechanosensitive ion channel from *E. coli*; Tb-MscL, large mechanosensitive ion channel from *M. tuberculosis*; GOF, gain of function; MEME, multiple EM for motif elicitation; AMPS, alignment of multiple sequences; PAGE, polyacrylamide gel electrophoresis; NHS, *N*-hydroxysuccinimide; DDM, *N*-dodecyl β-D-maltoside; EDC, 1-ethy-3-(3-dimethylaminopropyl)carbodiimide; DCC, *N*,*N*′-dicyclohexylcarbodiimide.

[2] G. Shapovalov and H. A. Lester, unpublished results.

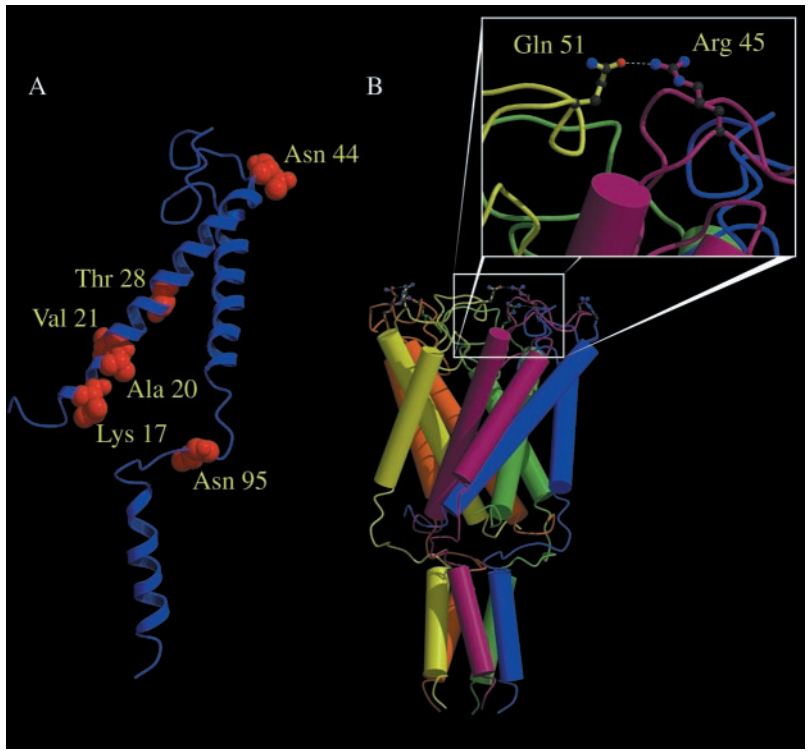

FIG. 1. ***M. tuberculosis* MscL crystal structure.** *A,* severe and very severe GOF mutations from Eco-MscL are mapped onto one subunit of the Tb-MscL crystal structure. *B,* the Arg^{45}–Gln^{51} hydrogen bond. The *box* shows a close-up of the hydrogen bond between the *yellow* and *purple* subunits. Figures were generated with MOLSCRIPT and Raster3D (18, 19).

loop, carboxyl terminus, and transmembrane regions one and two, by using the helix definitions of Chang *et al*. (1). The extracellular loop is defined as the region between the first and second transmembrane domains, and the carboxyl terminus is the region from the end of the second transmembrane domain to the end of the carboxyl helix. Pairwise alignments of the various regions were performed using AMPS, and scores for each pair were summarized as contour plots. Scores reflect the alignment of sequence A to sequence B relative to a shuffled sequence B and are therefore corrected for length. Scores above 5 indicate very good alignment between two protein sequences; scores between 2 and 5 indicate moderate alignment, and scores below 2 indicate poor alignment.

Constructs, Strains, and Cell Growth—All mutations were generated from a pET 19b (Novagen) construct containing the *M. tuberculosis* MscL open reading frame (1) using the QuikChange Method (Stratagene). Mutations were confirmed by enzymatic digest and sequencing. Expression and growth studies were carried out in BL21(DE3) *E. coli* using an MscL knockout mutant (1). All bacterial growth was done in the presence of 100 μg/ml ampicillin.

Growth studies were carried out as described previously (14). Cells were grown in LB media to an A_{600} of approximately 0.6 and diluted to an A_{600} of 0.2 ± 0.02. The cells were further diluted to 10^{-3}, 10^{-4}, 10^{-5}, and 10^{-6} and spotted (5 μl) onto 12-well LB plates in the presence or absence of 1 mM isopropyl-1-thio-β-D-galactopyranoside. Plates were imaged and scored after 20 and 40 h. A scoring system was developed, in which the score for a given growth plate was incremented by one for each concentration in which growth was observed (maximum score of 4). A minimum of 11 replications from four separate dilutions were obtained for each mutant.

Protein expression was performed by growing cells to the midpoint of log phase and inducing with 0.1% isopropyl-1-thio-β-D-galactopyranoside and 1% lactose. Following induction, cells were grown for an additional 2 h, harvested, and solubilized in 1% DDM, 10 mM Tris, and 10 mM NaCl. Protein was purified on a nickel-chelation column (Qiagen) in the presence of 0.05% DDM. The resulting proteins were verified by MALDI-TOF mass spectral analysis.

Cross-linking Studies—Wild type or R45K/Q51E protein solubilized in DDM micelles was diluted to a concentration of approximately 25 μg/ml and cross-linked at 4 °C for 2 h using 10 mM EDC, 10 mM DCC, 10 mM EDC/10 mM Sulfo-NHS, or 10 mM DCC/10 mM NHS. All cross-linking reactions were quenched with SDS-PAGE loading buffer containing β-mercaptoethanol. Reaction products were run on 4–15% gradient polyacrylamide gels and visualized by Western blotting with either a His_6 antibody (Amersham Pharmacia Biotech) or INDIA His probe-horseradish peroxidase (Pierce). Cysteine cross-linking reactions were performed and assayed in a similar manner on wild type and R45C/Q51C Tb-MscL. Thioesters were formed with bismaleimide reagents (Pierce), or disulfide bonds were formed with 3 mM copper phenanthroline. For the copper phenanthroline studies β-mercaptoethanol was omitted from the loading buffer.

RESULTS

Sequence Analysis—Although clearly related, the mechanosensitive channels from various organisms show moderate to low sequence identities. For example, the sequence identity of Tb-MscL compared with Eco-MscL is 37%, whereas the sequence identity of *Bordatella bronchiseptica* MscL compared with *Mycobacterium leprae* MscL is 15%. Therefore, development of an optimal alignment is not straightforward. For this reason, we have augmented sequence alignment approaches with MEME analysis, looking for patterns of conservation across the series. Fig. 2 shows an AMPS multiple sequence alignment and MEME group analysis of 35 putative MscL sequences. The MEME group analysis was used to make slight adjustments to the AMPS multiple sequence alignment using the indicated areas of conservation within the sequences. This alignment was further analyzed to determine which regions of MscL were most divergent using AMPS pairwise alignment of the full sequences and also of selected regions such as the first and second transmembrane domains, the extracellular loop, and the carboxyl terminus. Regional divisions were made by applying the previous definitions from the Tb-MscL crystal structure to the multiple sequence alignment (1). These alignments indicate general overall similarity for all regions of the protein; however, the loop region clearly shows the most variability. Contour plots showing scores for the AMPS pairwise alignments of the first transmembrane domain, the extracellular loop, and the carboxyl terminus are shown in Fig. 3.

Mutational Mapping—With an optimal alignment in hand (Fig. 2), we were able to map some of the very severe and severe mutations from Eco-MscL (11, 14) onto Tb-MscL. The most extensively probed type of mutation has been the so-called gain of function (GOF) mutation. This is observed in growth studies

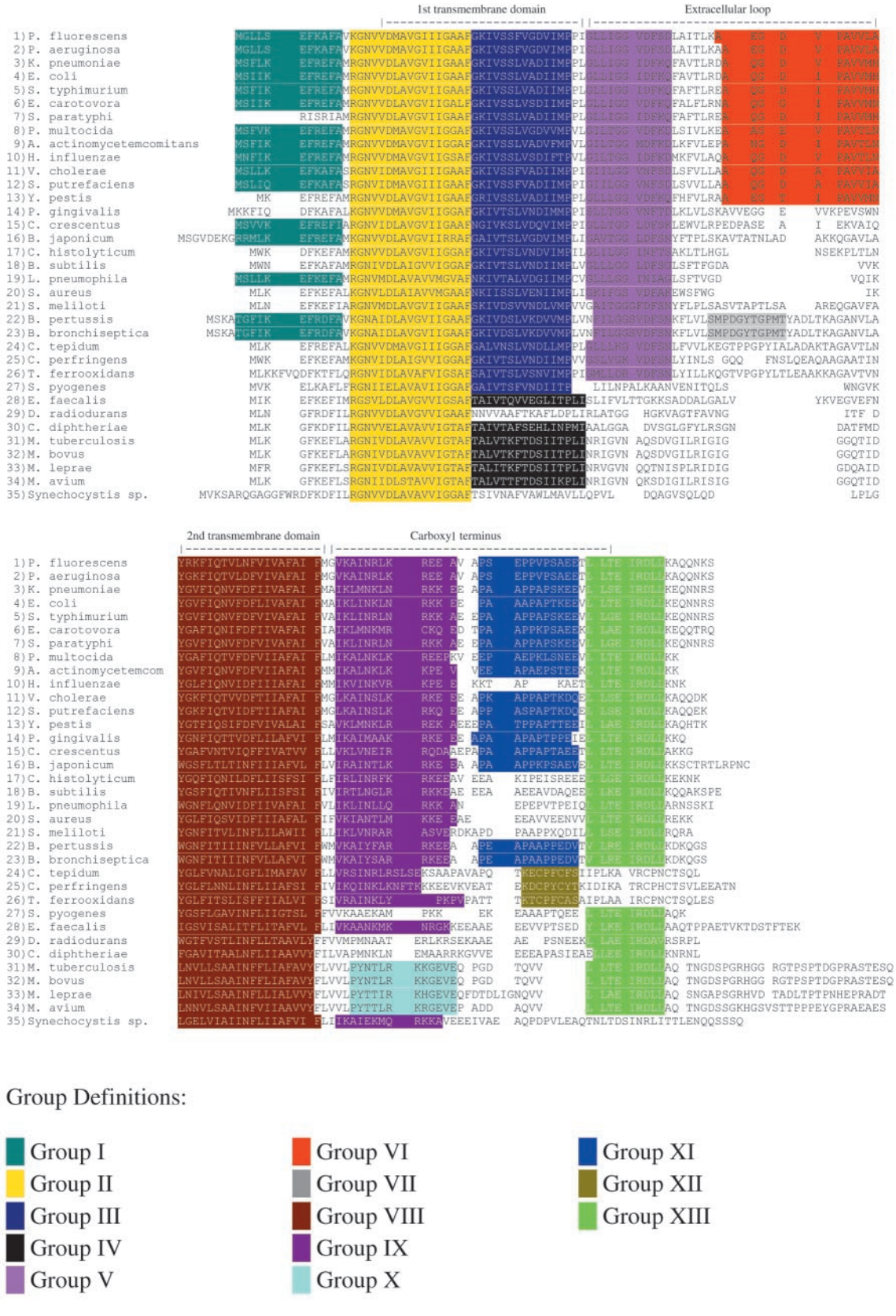

FIG. 2. **MEME consensus group analysis shown on the AMPS multiple sequence alignment.** The AMPS multiple sequence alignment of 35 putative MscL sequences is shown. The *colored regions* on the sequence alignment indicate MEME consensus groups.

of *E. coli* expressing the mutant channel. It is assumed that a mutation that increases channel opening probability will, in effect, put a hole in the cell membrane, which is deleterious to growth. The screen thus identifies channels that have a higher open probability at ambient pressure, which is considered a gain of function (9, 11, 14).

Fig. 1*A* shows the positions of these mutationally sensitive sites mapped onto the Tb-MscL structure. In all cases the

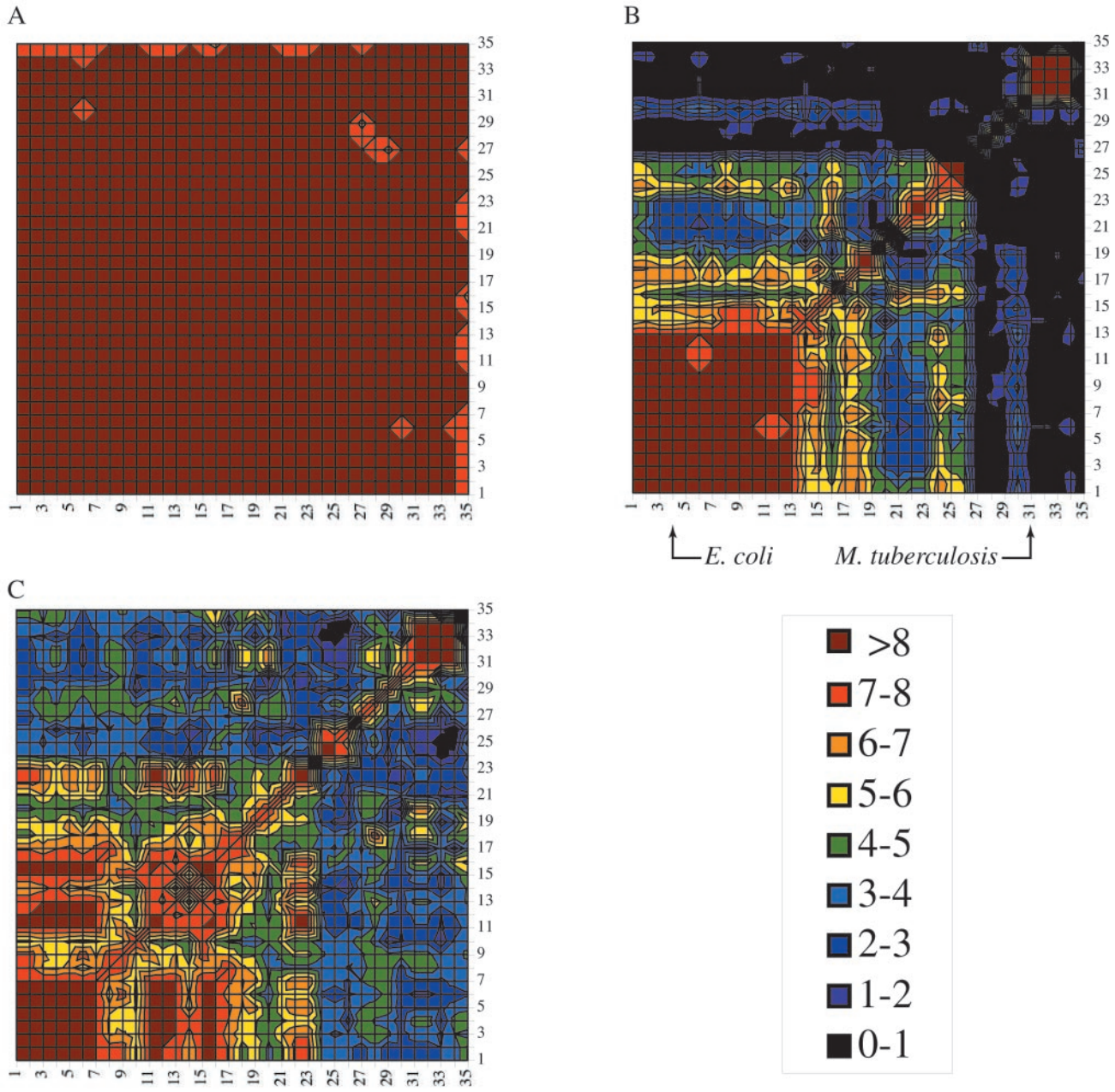

FIG. 3. **Regional AMPS pairwise alignments for the first transmembrane domain, the loop region, and the carboxyl terminus.** *Numbers* on axes correspond to the sequence numbers in Fig. 2. *A,* the contour plot for the first transmembrane domain shows that this region of the MscL protein is almost completely conserved. *B,* the loop region shows much more diversity than seen in the first transmembrane domain. Very low scores are observed for some pairs of proteins in this region. The contour plot shows groupings of sequences, with a large subfamily containing *E. coli* and a smaller subfamily containing *M. tuberculosis. C,* the contour plot of the carboxyl-terminal region shows more diversity than observed for the first transmembrane domain but less diversity than observed for the loop region.

alignment we obtain for these residues is the same as others have reported previously (1, 3, 5, 6). Site-directed mutagenesis of Tb-MscL at these positions was performed, converting the wild type amino acid to a residue shown in *E. coli* to give a GOF phenotype. The resulting mutations were analyzed using plate growth studies and scored using the system described under "Materials and Methods." Typical plate growth results are shown in Fig. 4, and all results are gathered in Table I. A GOF phenotype was observed in L17Y, V21A, N44D, and N95D. Unexpectedly, normal growth was observed for A20E, A20R, and T28R, even though the aligned positions, especially Ala^{20}, were shown to be very sensitive to mutation in Eco-MscL (11, 12, 14). That mutants displaying normal growth were indeed expressing a MscL channel was verified by SDS-PAGE analysis and Western blotting, which showed levels of protein expression within the variation seen for wild type Tb-MscL.

Tb-MscL Loop Intersubunit Hydrogen Bond—Examination of the Tb-MscL structure revealed an intersubunit hydrogen bond, Arg^{45}–Gln^{51}, located in the loop region of the channel (Fig. 1*B*). Suspecting that such a specific intersubunit contact may be important to function, we mutated this interaction to R45K/Q51E and R45C/Q51C to determine the proximity of these residues under physiological conditions by cross-linking analysis. The R45K/Q51E mutation was overexpressed and purified from *E. coli*. Cross-linking studies were performed in DDM micelles using EDC or DCC, with or without NHS activators. A typical SDS-PAGE Western blot of cross-linking products is shown in Fig. 5. Cross-linking is always seen, and in

some cases it is quite efficient. After treatment with 10 mM EDC and 10 mM sulfo-NHS, the majority of the observed cross-linked product is tetrameric or pentameric, establishing the high efficiency of this rationally designed cross-linking system. Cross-linking of the R45C/Q51C mutant produced similar results to the standard cross-linking of the salt-bridge mutant, but in no instance was highly efficient formation of tetramer and pentamer seen.

Since cross-linking studies confirmed the close proximity of Arg^{45} and Gln^{51} under physiological conditions, growth studies were used to assess the effects of mutations at these positions on channel function. The results of growth studies for some single and double mutants at these positions are summarized in Table II. All mutations at these positions, with the exception of R45K/Q51K, show a GOF phenotype.

DISCUSSION

Sequence Analysis—The MEME sequence analysis has provided insight into the overall similarity of the MscL homologues. Not surprisingly, the homologues are most similar in the transmembrane regions and most divergent in the loop and carboxyl-terminal regions. The strong similarities in the transmembrane domains are highlighted by the fully conserved groups, II and VIII, and the highly conserved group III. Additionally, members of the MscL family that lack group III in the first transmembrane region tend to have a similar conserved group IV in this region.

The carboxyl-terminal and loop region are much less conserved. Despite the appearance of three consensus groups in the loop region, V, VI, and VII, these groups are clearly not universal. The carboxyl terminus is more highly conserved than the loop region, but it is clearly not as well conserved as the transmembrane helices. The carboxyl terminus contains two very highly conserved groups, IX and XIII, and the less conserved group XI. Mycobacteria do not contain group IX, but an analogous charged region is evident (group X). Previously it has been shown that a large portion of the carboxyl terminus in Eco-MscL can be deleted without affecting protein function (15). This is consistent with the lack of sequence conservation in this region.

To examine further the similarities and differences among MscL homologues, a pairwise alignment of the various regions was employed (Fig. 3). The pairwise alignments showed the same general trends observed with MEME analysis. In general, all regions of the MscL sequence are conserved; however, the loop region has pairs of sequences with poor alignment. To some extent the sequence pairs within the loop region can be used to group the homologues into subfamilies. The largest and most obvious subfamily includes *E. coli* MscL and other sequences containing MEME group VI. Another distinctive subfamily includes the Mycobacteria. Thus, by this analysis Eco-MscL and Tb-MscL are in different subfamilies.

Mutational Mapping—Previous mutational analysis of Eco-MscL has focused mainly on the highly conserved transmembrane regions, with only a few randomly obtained mutations in the loop (9, 11, 12, 14, 15). For the transmembrane regions, one would expect the sequence homology mapping of the previously obtained GOF *E. coli* mutants onto Tb-MscL to give mutants with a GOF phenotype, due to the high sequence homology in these regions. Note that all alignments, the one reported here and those published previously, agree as to which residues in Tb-MscL correspond to previously studied GOF sites in Eco-MscL (1, 3, 5, 6).

For the majority of mutations studied (L17Y, V21A, N44D, and N95D), the GOF phenotype seen in Eco-MscL is also seen in Tb-MscL (Table I and Fig. 4). Surprisingly, however, mutations at Ala^{20} and Thr^{28} do not yield a GOF phenotype. The

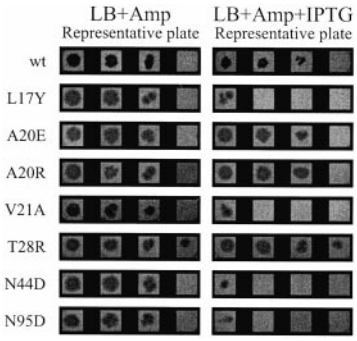

FIG. 4. **Representative plate growth for mutations mapped from *E. coli* MscL to *M. tuberculosis* MscL.** The *left panel* shows the uninduced control, and the *right panel* shows growth in the presence of isopropyl-1-thio-β-D-galactopyranoside (*IPTG*). In both panels samples were plated (*left* to *right*) from high concentration to low concentration. A GOF phenotype is observed for L17Y, V21A, N44D, and N95D. No difference from wild type growth is seen for A20E, A20R, and T28R.

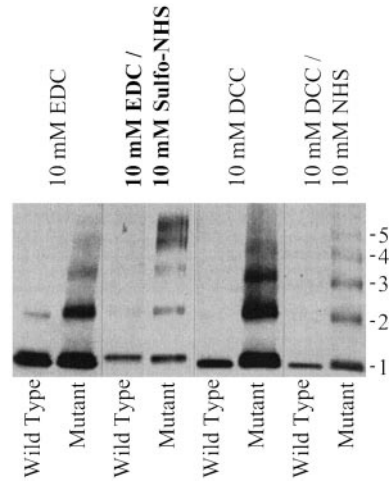

FIG. 5. **Cross-linking of the R45K/Q51E mutant of *M. tuberculosis* MscL.** Purified R45K/Q51E *M. tuberculosis* MscL and wild type protein were cross-linked for 2 h at 4 °C using EDC, DCC, EDC with sulfo-NHS, and DCC with NHS. The reactions were quenched with β-mercaptoethanol, run on a 4–15% SDS-polyacrylamide gel, and visualized by Western blotting with His_6 antibody.

TABLE I
Summarized growth data for GOF mutants mapped from E. coli MscL to M. tuberculosis MscL

Mutant	Number of plates		Average score after 20 h		Average score after 40 h	
	Uninduced	Induced	Uninduced	Induced	Uninduced	Induced
Wild type	51	52	3.38	2.64	3.29	2.75
L17Y	11	11	3.10	0.70	3.19	0.70
A20E	13	13	3.38	3.47	3.38	3.47
A20R	13	13	3.32	3.52	3.32	3.52
V21A	11	11	2.85	1.10	2.85	1.10
T28R	13	13	3.79	3.47	3.79	3.47
N44D	11	11	3.27	0.57	3.27	0.57
N95D	11	11	3.12	0.20	3.20	0.60

TABLE II
Summarized growth data for mutations of the Arg-45/Gln-51 hydrogen bond in M. tuberculosis MscL

Mutant	Number of plates		Average score after 20 h		Average score after 40 h	
	Uninduced	Induced	Uninduced	Induced	Uninduced	Induced
K45/E51	12	13	3.57	0.00	3.14	0.00
R45K	12	12	3.35	0.00	3.35	0.00
Q51E	12	12	3.07	0.00	3.07	0.00
E45/E51	14	14	3.26	0.64	3.26	0.64
K45/K51	14	14	3.41	3.00	3.62	3.14
C45/C51	12	13	3.65	0.27	3.29	0.43
R45C	12	12	3.59	0.00	3.59	0.00
Q51C	12	12	3.56	0.00	3.56	0.00

production of Tb-MscL protein for these mutants was confirmed by SDS-PAGE analysis. The lack of GOF phenotype for the A20E and A20R mutants is particularly surprising in light of recent work (14), which shows that all charged residues at this site give a very severe GOF phenotype in Eco-MscL. In fact, only Ala and Gly at these sites produce Eco-MscL with normal function (12).

Tb-MscL Loop Intersubunit Hydrogen Bond—Previous studies of mutations at Gly^{46} in Eco-MscL showed the GOF phenotype (11). We have seen similar behavior at the aligned Asn^{44} site in Tb-MscL. On examining the Tb-MscL crystal structure, we observed an inter-subunit hydrogen bond involving the adjacent Arg^{45} site, with Gln^{51} serving as the partner (Fig. 1*B*). This significant intersubunit interaction suggested an interesting starting point to explore loop function.

Initially, the intersubunit hydrogen bond in the crystal structure was mutated to cross-linkable residues to examine whether these residues are in close proximity under more physiological conditions. The subtle mutation of R45K/Q51E converts the hydrogen bond to a salt bridge. This should still be a favorable intersubunit contact, but the mutant is now susceptible to cross-linking by peptide bond-forming reagents. After overexpression and purification, the protein was exposed to a variety of cross-linking reagents and activators for 2 h at 4 °C. All reagents showed at least a weak pentameric band in the mutant with slight background cross-linking in wild type (Fig. 5). The background cross-linking is most likely due to cross-linking in the carboxyl terminus of the protein, which contains a number of glutamates, aspartates, and lysines.

The most interesting cross-linking results were seen with EDC and Sulfo-NHS. This combination gives mainly pentamer and tetramer for cross-linked products. The strong pentameric band in this designed system provides the best evidence to date that Tb-MscL is pentameric under physiological conditions. Other cross-linking studies typically show progressively weaker band intensities on going from monomer to dimer to trimer, etc., analogous to our results with just EDC and other non-optimal conditions (Fig. 5) (24–26). Such observations always leave open the possibility that a hexamer band is present but is too weak to be seen as the intensity progressively falls off with higher oligomerization. Under some conditions, a weak band assigned to hexamer has been seen. However, with the designed double mutant under appropriate conditions (EDC/Sulfo-NHS), very strong tetramer and pentamer bands are seen, but no hexamer band is visible. This provides compelling evidence that no significant fraction of Tb-MscL is present in hexameric (or higher oligomerization) states when reconstituted in DDM micelles.

After confirming that the residues Arg^{45} and Gln^{51} were within interaction distance, we performed growth studies on both single and double mutants to examine channel function. All single mutants (R45K, Q51E, R45C, and Q51C) and all double mutants (R45K/Q51E, R45E/Q51E, and R45C/Q51C) except R45K/Q51K displayed a GOF phenotype (Table II). The lack of a GOF phenotype for the R45K/Q51K mutant is surprising and merits further study. Nevertheless, this region appears to be quite mutationally sensitive. Note that the R45K mutation is subtle, suggesting that the loop plays a central role in channel gating. Very recently it has been shown that proteolytic cleavage of the loop significantly alters channel gating (16), supporting our view of a critical functional role for this region.

By using the alignment of Fig. 2, there is no obvious Eco-MscL analogue to the Arg^{45}–Gln^{51} hydrogen bond seen in Tb-MscL. Technically, the alignment is Leu^{47}/Asp^{53} (Eco-MscL numbering), which is not a favorable interaction. There is no cationic or hydrogen bond donating residue near Leu^{47} that could pair with Asp^{53}. However, residues on either side of Asp^{53} are hydrophobic, suggesting that perhaps the ion pair of Tb-MscL is replaced by a hydrophobic contact such as Leu^{47}/Ile^{52} or Leu^{47}/Phe^{54} in Eco-MscL. It would be interesting to investigate this possibility.

These studies suggest that although *M. tuberculosis* and *E. coli* MscL are similar, there are important differences. Thus, caution should be exercised when employing the Tb-MscL crystal structure to explain functional results for Eco-MscL. Most strikingly, mutations at Ala^{20} in Tb-MscL do not exhibit a GOF phenotype, despite the extreme sensitivity of the aligned Gly^{22} in *E. coli*. Additionally, the loop region of Tb-MscL appears highly sensitive to mutations, suggesting that the loop region in general and the Arg^{45}–Gln^{51} intersubunit hydrogen bond in particular, merit further investigation.

Acknowledgments—We are grateful to Prof. Douglas Rees, Dr. Randal Bass, Dr. Geoffrey Chang, Dr. Robert Spencer, and George Shapovalov for helpful discussions. Plasmids and wild type Tb-MscL proteins used in these studies were obtained from the Rees group. MALDI-TOF mass analyses were carried out at the Caltech Protein Microanalytical Laboratory under the direction of Gary M. Hathaway.

REFERENCES

1. Chang, G., Spencer, R. H., Lee, A. T., Barclay, M. T., and Rees, D. C. (1998) *Science* **282,** 2220–2226
2. Doyle, D. A., Cabral, J. M., Pfuetzner, R. A., Kuo, A. L., Gulbis, J. M., Cohen, S. L., Chait, B. T., and MacKinnon, R. (1998) *Science* **280,** 69–77
3. Batiza, A. F., Rayment, I., and Kung, C. (1999) *Struct. Fold. Des.* **7,** R99–R103
4. Blount, P., and Moe, P. C. (1999) *Trends Microbiol.* **7,** 420–424
5. Oakley, A. J., Martinac, B., and Wilce, M. C. J. (1999) *Protein Sci.* **8,** 1915–1921
6. Spencer, R. H., Chang, G., and Rees, D. C. (1999) *Curr. Opin. Struct. Biol.* **9,** 448–454
7. Rees, D. C., Chang, G., and Spencer, R. H. (2000) *J. Biol. Chem.* **275,** 713–716
8. Sukharev, S., Durell, S. R., and Guy, H. R. (2000) *Biophys. J.* **78,** A473
9. Blount, P., Schroeder, M. J., and Kung, C. (1997) *J. Biol. Chem.* **272,** 32150–32157
10. Blount, P., Ou, X., Hoffman, R. J., and Kung, C. (1998) *Biophys. J.* **74,** A324
11. Ou, X. R., Blount, P., Hoffman, R. J., and Kung, C. (1998) *Proc. Natl. Acad. Sci. U. S. A.* **95,** 11471–11475
12. Batiza, A. F., and Kung, C. (2000) *Biophys. J.* **78,** A473
13. Liu, W., Deitmer, J. W., and Martinac, B. (1999) *Biophys. J.* **76,** A203
14. Yoshimura, K., Batiza, A., Schroeder, M., Blount, P., and Kung, C. (1999)

Biophys. J. **77,** 1960–1972
15. Blount, P., Sukharev, S. I., Schroeder, M. J., Nagle, S. K., and Kung, C. (1996) *Proc. Natl. Acad. Sci. U. S. A.* **93,** 11652–11657
16. Ajouz, B., Berrier, C., Besnard, M., Martinac, B., and Ghazi, A. (2000) *J. Biol. Chem.* **275,** 1015–1022
17. Moe, P. C., Levin, G., and Blount, P. (2000) *Biophys. J.* **78,** A137
18. Kraulis, P. J. (1991) *J. Appl. Crystallogr.* **24,** 946–950
19. Merritt, E. A., and Bacon, D. J. (1997) *Methods Enzymol.* **277,** 505–524
20. Barton, G. J., and Sternberg, M. J. E. (1987) *J. Mol. Biol.* **198,** 327–337
21. Barton, G. J. (1990) *Method Enzymol.* **183,** 403–428
22. Bailey, T. L., and Elkan, C. (1995) *Proceedings of the 2nd International Conference on Intelligent Systems for Molecular Biology, Palo Alto, CA*, 1994 (Altman, R., ed) pp. 28–36, AAAI Press, Menlo Park, CA
23. Bailey, T. L., and Gribskov, M. (1998) *Bioinformatics* **14,** 48–54
24. Blount, P., Sukharev, S. I., Moe, P. C., Schroeder, M. J., Guy, H. R., and Kung, C. (1996) *EMBO J.* **15,** 4798–4805
25. Sukharev, S. I., Schroeder, M. J., and McCaslin, D. R. (1999) *J. Membr. Biol.* **171,** 183–193
26. Hase, C. C., Minchin, R. F., Kloda, A., and Martinac, B. (1997) *Biochem. Biophys. Res. Commun.* **232,** 777–782